^{26}Al(n,p_1) and (n,α_0) cross sections from thermal energy to 70 keV and the nucleosynthesis of ^{26}Al

P. E. Koehler,[1] R. W. Kavanagh,[2] R. B. Vogelaar,[3] Yu. M. Gledenov,[4] and Yu. P. Popov[4]
[1]*Physics Division, Oak Ridge National Laboratory, Oak Ridge, Tennessee 37831-6354*
[2]*W. K. Kellogg Radiation Laboratory, California Institute of Technology, Pasadena, California 91125*
[3]*Princeton University, Department of Physics, Princeton, New Jersey 08544*
[4]*Laboratory of Neutron Physics, Joint Institute for Nuclear Research, Dubna, Russia*
(Received 31 March 1997)

We have measured the ^{26}Al$(n,\alpha_0)^{23}$Mg and ^{26}Al$(n,p_1)^{26}$Mg* cross sections from thermal energy to approximately 10 keV and 70 keV, respectively. These reactions are thought to be the major mechanisms for the destruction of ^{26}Al in many nucleosynthesis environments; hence, an accurate determination of their rates is important for understanding the observations of γ rays from ''live'' ^{26}Al in our galaxy and of ''extinct'' ^{26}Al in meteorites. The astrophysical rate for the ^{26}Al$(n,\alpha_0)^{23}$Mg reaction determined from our measurements is in good agreement with the rate determined via inverse measurements. On the other hand, the rate we determined for the ^{26}Al$(n,p_1)^{26}$Mg* reaction is significantly larger than previously reported. In addition, we were able to determine this rate in the temperature range below 0.2 GK which was not covered by previous measurements. This lower temperature range may be important for understanding the production of ^{26}Al in Red Giant stars. Both of our rates are significantly different than the rates used in most nucleosynthesis calculations. We discuss the impact of our measurements on the nucleosynthesis of ^{26}Al. [S0556-2813(97)07208-7]

PACS number(s): 25.40.Hs, 26.20.+f, 26.35.+c, 27.30.+t

I. INTRODUCTION

The origin and subsequent history of radioactive ^{26}Al is exceedingly interesting to astrophysics because it is a potentially valuable probe of stellar nucleosynthesis, of galactic chemical evolution, and of the formation of the solar system. This is because both ''extinct'' ^{26}Al has been observed in meteorites and the distribution of ''live'' ^{26}Al has been mapped in our galaxy, and because the production of ^{26}Al appears to be ubiquitous in many nucleosynthesis models.

The presence of extinct ^{26}Al in Ca-Al-rich inclusions in meteorites [1–3] was inferred from observations of material having anomalously high ^{26}Mg/^{24}Mg ratios but essentially solar ^{25}Mg/^{24}Mg. In addition, a correlation was found between the amount of aluminum in the inclusion relative to magnesium and the size of the ^{26}Mg anomaly. Therefore, it was concluded that ^{26}Al was alive when the inclusions formed and that its subsequent decay gave rise to anomalous ^{26}Mg. This and other isotopic anomalies in meteorites have been interpreted as evidence, for example, that the formation of the solar system was aided by the explosion of a nearby supernova [4], or by mass ejection from a nearby red giant star during its most active phase [5].

The first observation of ''live'' ^{26}Al outside the solar system [6] was made using the HEAO3 satellite which detected the 1.809 MeV γ ray resulting from the decay of ^{26}Al to the first excited state of ^{26}Mg. Subsequently, the distribution of ^{26}Al in the galaxy has been mapped using instruments on the Compton Gamma-Ray Observatory (CGRO) [7]. These observations provide a unique diagnostic of relatively recent (and almost certainly ongoing) nucleosynthesis. Because these observations of ^{26}Al are unique and detailed, they present both a challenge to nuclear astrophysics and a hope that such data will lead to significant advances.

Many different sites have been proposed as the birthplace of ^{26}Al. These include presupernova and supernovae nucleosynthesis in massive stars [8–12], Asymptotic Giant Branch (AGB) stars [5,13–15], Wolf-Rayet (W-R) stars [16,17], cosmic rays [18,19], and novae [20–23]. The CGRO observations appear to indicate that massive stars are the most likely source of the bulk of the ^{26}Al in our galaxy. Calculations have shown that neutron-induced reactions, most notably ^{26}Al(n,p), are the main route for the destruction of ^{26}Al in many scenarios involving massive stars. In addition, these same reactions are calculated to destroy a sizable fraction of the ^{26}Al synthesized in AGB stars. In these environments, the amount of ^{26}Al produced is roughly inversely proportional to the ^{26}Al(n,p) reaction rate; hence, it is important that this rate be determined accurately.

The ^{26}Al(n,p_0) and ^{26}Al(n,α_0) (where a subscript 0, 1, etc., designates the reaction in which the residual nucleus is left in the ground state, first excited state, etc.) reaction rates were first determined via detailed balance using measurements of the cross sections for the inverse reactions [24,25]. The reaction rates determined from these measurements were very different from the theoretical predictions [26]. For example, theory predicted that the (n,p) would be much larger than the (n,α) rate, whereas the measured (n,α_0) rate was much larger than the (n,p_0) rate. Based on these measurements, the level density in ^{27}Al was revised downward to obtain an improved (n,p) reaction rate [27] which was a factor of 3.3 lower than the previous one, but still about a factor of 10 larger than the measured (n,p_0) rate.

Based on the spins of the levels involved, it was speculated [24] that the ^{26}Al(n,p_1) cross section, which is not measurable via the inverse reaction, would be larger than that

for the (n,p_0) reaction. This expectation was verified in the first direct measurement of these cross sections [28] in which it was determined that the $(n,p_1)/(n,p_0)$ ratio varies from approximately 100 at thermal energy to about 3 near 300 keV. At astrophysically relevant energies the improved theoretical rate [27] was still 50% higher than the measured one [28]. However, the measurements of Ref. [28] were made with a neutron source which approximates, but does not exactly reproduce, a Maxwell-Boltzmann distribution at kT=31 and 71 keV. The extent to which this approximation affects the reaction rate extracted from the measurements depends on the energy dependence of the cross section. However, the measurements of Ref. [28] were made only at four widely spaced energies, so the energy dependence of the cross section was not well constrained by these data. In addition, the reaction rate was not determined for temperatures in the range kT=40×10^{-6} to 31 keV although the data indicate that the rate changes by a factor of 63 across this region. Hence, the temperature range typical of neutron exposure in AGB stars (kT=6 to 23 keV) was left undetermined. Also, the cross section for the ^{26}Al(n,α) reaction was not measured in Ref. [28]. Finally, measurements of the ^{14}N$(n,p)^{14}$C [29] and ^{7}Li$(n,\gamma)^{8}$Li [30] cross sections using a technique very similar to that used in Ref. [28] are in serious disagreement with other measurements [31–34] using different techniques. For these reasons, new measurements were desired. We have measured the ^{26}Al(n,α_0) and ^{26}Al(n,p_1) cross sections from thermal energy to approximately 10 keV and 70 keV, respectively. This energy range provides sufficient overlap to check previous measurements and allows the reaction rates in the low temperature region characteristic of AGB stars to be determined.

II. EXPERIMENTAL PROCEDURES

The measurements were performed at the moderated ''white'' neutron source of the Los Alamos Neutron Science Center (LANSCE) [35] using an apparatus which has been described elsewhere [36] so only the salient details will be mentioned herein.

The ^{26}Al for the samples was produced by spallation at the Los Alamos Meson Physics Facility (LAMPF) using an electronics-grade silicon target. The LAMPF material had an isotope ratio of ^{27}Al/^{26}Al$\approx$16. The samples were made [37] by vacuum evaporation of a carbon-aluminum oxide-carbon sandwich onto a copper backing foil which was 76 μm thick. During preliminary measurements it was found that the copper backing caused unacceptably large background and large dead time at short time-of-flight, so it was etched away and the sample was supported by a smaller niobium foil which was 25 μm thick. The sample deposit was approximately 0.4 cm in diameter whereas the neutron beam was about 0.7 cm in diameter at the sample position. Most of the measurements were made with a sample containing approximately 4×10^{15} atoms of ^{26}Al. A few measurements were made with a sample containing about 2.6×10^{15} atoms of ^{26}Al. These latter measurements were used as a check on the energy calibration of the pulse-height spectra to ensure that the peaks due to the ^{26}Al(n,p_1) and ^{26}Al(n,α_0) reactions were identified correctly.

Reaction products were detected with a silicon surface-barrier detector telescope comprised of a ΔE detector which was 50 μm thick by 300 mm^2 followed by an E detector which was 50 μm thick by 450 mm^2. The detectors were placed at 90° to the neutron beam at about 3 cm from the center of the sample. The solid angles subtended by the detectors were determined using a calibrated ^{241}Am source. Small corrections to the measured solid angles, due to the fact that the area of the ^{241}Am source was smaller than the area of the sample, were calculated using Monte Carlo techniques. The coincidence timing spectrum between the detectors was measured using a Time-to-Amplitude Converter (TAC). The coincidence timing peak had a FWHM of about 31 ns and a width of about 150 ns at its base. For each event in the ΔE detector, the neutron time-of-flight, the pulse heights in the two detectors, and the TAC spectrum were written to disk. Several spectra were displayed ''on-line'' to monitor the progress of the experiment. The data were replayed ''off-line'' to obtain the final yields. The gate on the $\Delta E-E$ coincidence timing spectrum was set to approximately 1μs width to ensure that all coincidence events were recorded. The ΔE and E pulse-height spectra were calibrated using measurements on ^{6}Li$(n,\alpha)^{3}$H, ^{10}B$(n,\alpha)^{7}$Li, and ^{41}Ca$(n,\alpha)^{38}$Ar. The ΔE versus E spectrum for all neutron energies between thermal and 70 keV (a total of 823 counts) is shown in Fig. 1. As can be seen, a peak due to the ^{26}Al(n,p_1) reaction was observed with a very good signal-to-noise ratio.

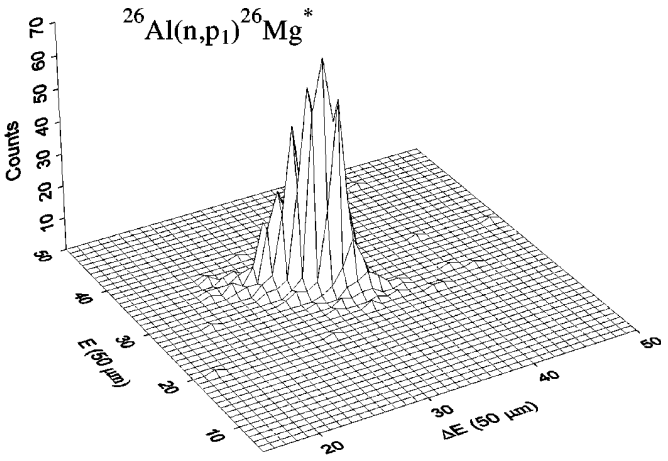

FIG. 1. Pulse-height spectrum from our ^{26}Al(n,p) measurements.

The measurements were made relative to the ^{6}Li$(n,\alpha)^{3}$H cross section using a separate ^{6}Li sample and solid-state detector as a flux monitor. The data were converted from yields to cross sections using the latest evaluation for the ^{6}Li$(n,\alpha)^{3}$H cross section [38] and the measured ^{26}Al(n,p_1) cross section at 40 meV [28]. We chose to normalize our results using this latter value (rather than one of the other energy-cross section pairs reported in Ref. [28]) because it is the only one whose energy range fully overlaps the range of our data. Other reasons we chose this point for normalization include: (1) It was the most accurate value reported, (2) Our data show that the cross section has a very smooth energy dependence in this region, and (3) The cross section should be isotropic at this energy. Our ^{26}Al(n,α_0) data were normalized to our ^{26}Al(n,p_1) data in the region of

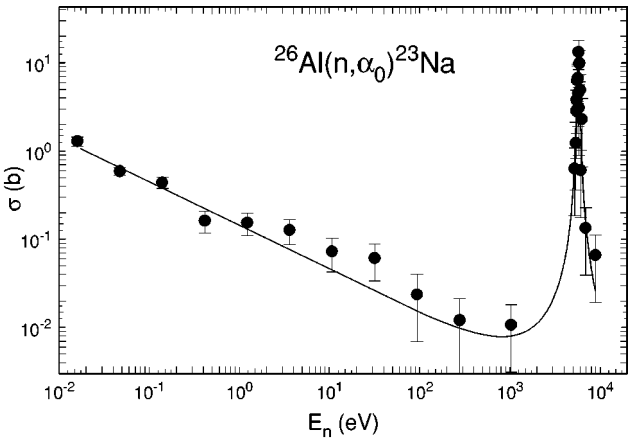

FIG. 2. The ^{26}Al$(n,\alpha)^{23}$Na cross sections between thermal energy and 10 keV. The circles with error bars are our data with one-standard-deviation statistical uncertainties. The curve is from a multilevel fit to the data as described in the text.

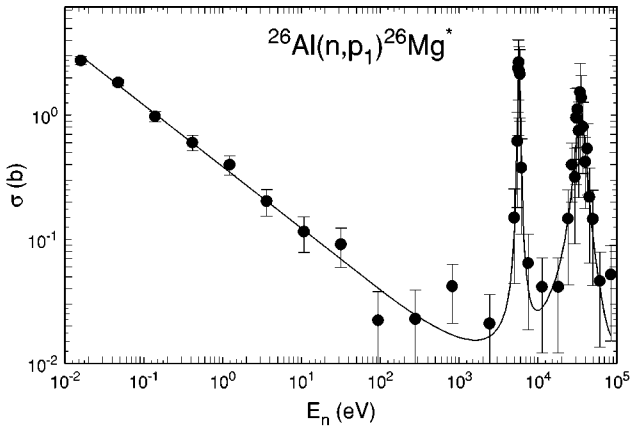

FIG. 3. The ^{26}Al$(n,p_1)^{26}$Mg cross sections between thermal energy and 70 keV. The circles with error bars are our data with one-standard-deviation statistical uncertainties. The curve is from a multilevel fit to the data as described in the text.

the resonance at 5.578 keV where the best signal-to-noise ratio was obtained in the former data. We assumed that the cross section was isotropic when converting our measured yields to cross sections. This assumption may not be valid at all energies because at least some of the resonances appear to be p wave as will be discussed below.

The data were taken at a source-to-sample distance of 7.026 m with a time-of-flight channel width of 2 ns. The data were analyzed using a minimum channel width of 32 ns. Below $E_n \approx$ 2 keV and between resonances, the data were compressed to improve the statistical precision. A separate run with a ^{6}Li sample in place of the ^{26}Al sample was used to determine the time-of-flight to energy calibration. Dips in the time-of-flight spectra due to resonances in aluminum and manganese in the various windows in the beam line were used for this calibration.

Because α-particles from the ^{26}Al(n,α_0) reaction were stopped in the ΔE detector, the background was much worse for this reaction and measurements were possible only below approximately 10 keV. In addition, to reduce dead-time effects as well as the background counting rate, the threshold on the ΔE detector was set too high to record protons from the ^{26}Al(n,p_0) reaction. This should not affect the usefulness of our data, however, because previous measurements [25,28] have shown that the cross section for other proton groups is much smaller than that for the p_1 group over the energy range of our measurements.

III. CROSS SECTIONS AND RESONANCE ANALYSIS

The ^{26}Al(n,α_0) and ^{26}Al(n,p_1) cross sections resulting from our measurements are shown in Figs. 2 and 3, respectively. The error bars depict the one-standard-deviation statistical uncertainties only. We calculate a normalization uncertainty of 8.3% for our ^{26}Al(n,p_1) data from the combined uncertainties in the ^{6}Li$(n,\alpha)^3$H and ^{26}Al(n,p_1) cross sections used to normalize our data. The normalization uncertainty in our ^{26}Al(n,α_0) data is much larger, approximately 26%, due to the additional uncertainty in the yield ratio for the 5.578 keV resonance.

A resonance at 5.578 keV appears to be the first in both reactions. In addition, there is a second resonance at 33.7 keV visible in the ^{26}Al(n,p_1) channel. An attempt was made to fit both cross sections from thermal energy to the maximum energy measured using only these two resonances assuming noninterfering Breit-Wigner shapes. The calculated resonance shapes were broadened to account for the resolution of the experiment as explained in Ref. [39]. The search was restricted to s wave ($J^\pi = \frac{9}{2}^+, \frac{11}{2}^+$) and p wave ($J^\pi = \frac{7}{2}^-$ to $\frac{13}{2}^-$) neutron resonances only, because the penetrabilities for higher partial waves are very small at these energies. It was not possible to fit both the thermal cross sections and the resonances at the same time. In particular, fitting the peaks using s wave resonances resulted in thermal cross sections that were much too large; hence, s wave assignments seem to be ruled out for both resonances unless there is significant interference between them and resonances outside our energy range. There are no levels in the compound nucleus ^{27}Al listed at this high an excitation energy ($E_x \geqslant$ 13.058 MeV) in the latest compilation [40]. For these reasons we refitted the data assuming both resonances were p wave and added $1/v$ components (presumably from an s wave resonance outside our energy range) which were fitted to the thermal cross sections. Good fits to the data could be

TABLE I. Resonance parameters.

		^{26}Al(n,p_1)		^{26}Al(n,α_0)	
E_{res} (keV)	Γ (eV)	$\sigma_{th}(b)$	$\omega\gamma$ (eV)	$\sigma_{th}(b)$	$\omega\gamma$ (eV)
-	–	2.37 ± 0.19	-	0.88 ± 0.23	-
5.578	240 ± 200	-	2.03 ± 0.51	-	6.6 ± 1.7
33.70	8200 ± 3000	-	128 ± 22	-	-

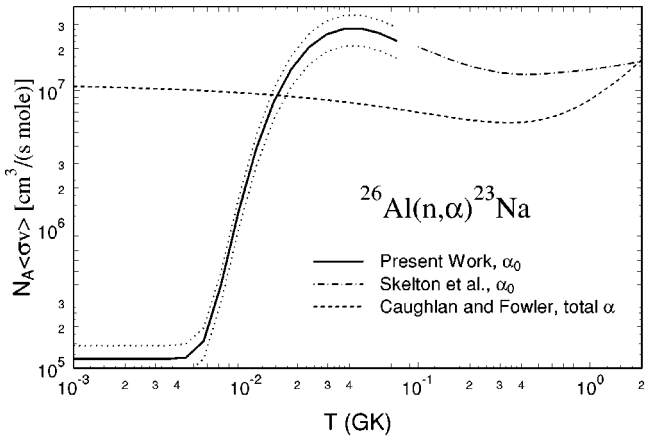

FIG. 4. The astrophysical reaction rate for ^{26}Al$(n,\alpha)^{23}$Na. The rate calculated from the multilevel fit to our data is shown as the solid curve with uncertainties depicted by the dotted curves. The rate from the inverse measurements of Ref. [25] is shown as a dashed-dotted curve whereas the statistical model calculation of the rate [27] is shown as the dashed curve.

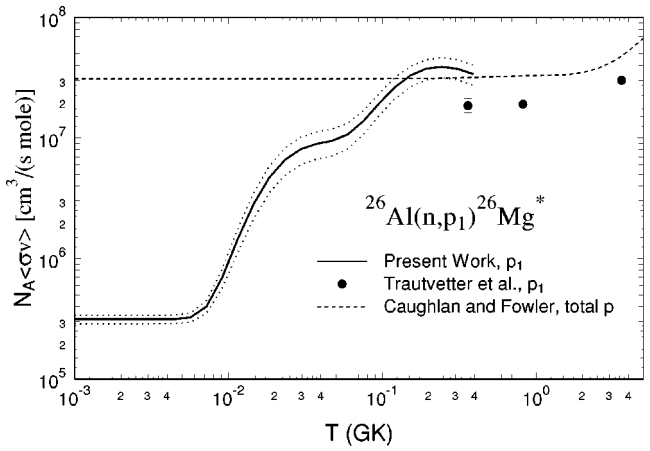

FIG. 5. The astrophysical reaction rate for ^{26}Al$(n,p)^{26}$Mg. The rate calculated from the multilevel fit to our data is shown as the solid curve with uncertainties depicted by the dotted curves. The rates from the previous measurements of Ref. [28] are shown as solid circles whereas the statistical model calculation of the rate [27] is shown as the dashed curve.

obtained under these assumptions as is shown in Figs. 2 and 3. The resonance parameters are listed in Table I.

The astrophysical reaction rates $N_A\langle\sigma v\rangle$, calculated from these resonance parameters following the prescription in Ref. [41], are shown in Figs. 4 and 5 as a function of temperature. The reaction rates calculated in this way are in agreement to within the experimental uncertainties with the rates calculated by numerically integrating the data. The uncertainties in our rates, depicted by the dotted curves in Figs. 4 and 5, were calculated from the normalization uncertainties given above plus the uncertainties in the resonance strengths. Because our measurements were made over a limited range of energies, above some temperature the rates calculated from our data can be considered only as lower limits. This temperature limit depends on the shape of the cross sections at energies above our measurements. Using previous measurements at higher energies [25,28] and theoretical estimates of the rates [27], we estimate that the rates calculated from our data are reliable up to approximately 0.08 GK for the ^{26}Al(n,α_0) reaction and 0.3 GK for the ^{26}Al(n,p_1) reaction. Our data for the ^{26}Al(n,p_1) reaction fill in the temperature range typical of the destruction of ^{26}Al via exposure to neutrons in AGB stars. Our data for both reactions define how the rates increase by a factor of 100 or more over the range from very low temperatures to temperatures typical of nucleosynthesis calculations.

IV. COMPARISON TO PREVIOUS WORK

Our results are compared to previous ^{26}Al(n,α_0) [25] and ^{26}Al(n,p_1) [28] measurements as well as statistical model calculations [27] in Figs. 4 and 5. Our results for the energy and strength of the 5.578 keV resonance agree with those of Ref. [25] to within the experimental uncertainties. This good agreement lends confidence to the normalization used in the present work and to our assumption that angular distribution effects can be neglected. Also, the energy of the first resonance observed in the ^{26}Al(n,p_0) channel in Ref. [25] is in good agreement with the energy of the second resonance we observe in the ^{26}Al(n,p_1) reaction.

Because the measurements of Ref. [28] (except for the lowest energy point which we used to normalize our data) were made with a source having a broad distribution extending to energies above our range, it is not possible to compare the two results directly as cross sections. Instead, our results are compared to those of Ref. [28] as reaction rates in Fig. 5. Unfortunately, there is very little overlap between the two measurements in such a comparison. However, our data indicate that the reaction rate is about a factor of two larger than the rate determined in Ref. [28]. There are several possible reasons for this disagreement.

First, all but the lowest energy measurements of Ref. [28] were made using a source whose flux and energy distributions vary significantly across the surface of the sample. This could lead to systematic errors due to sample nonuniformities. In contrast, our measurements were made using a uniform beam which was larger than the sample.

Second, in Ref. [28], the flux was determined by activation of a gold foil. However, the ^{197}Au(n,γ) cross section increases by a factor of about 175 between 30 keV and thermal energy whereas the ^{26}Al(n,p_1) cross section changes by a factor of only 15 or less. Therefore, a small ($\sim$1% or less) thermal component to the neutron flux (from moderation in walls, nearby equipment, etc.) could lead to a factor of two reduction in the measured ^{26}Al(n,p_1) cross section relative to ^{197}Au(n,γ) at 30 keV. Measurements of the ^{14}N$(n,p)^{14}$C [29] and ^{7}Li$(n,\gamma)^{8}$Li [30] cross sections using a technique very similar to that used in Ref. [28] are also a factor of 2–3 lower than the results from other measurements [31–34] using different techniques. In contrast, previous measurements of the ^{17}O$(n,\alpha)^{14}$C [42,43] and ^{36}Cl$(n,p)^{36}$S [44,45] at LANSCE and at Karlsruhe are, generally, in good agreement. Also, other results from LANSCE [[31,36,44,46,47], using techniques similar to the present work, are in agreement with data taken using several other methods [48–56].

Third, all but the lowest energy measurements of Ref. 28 were made by detecting reaction products over a relatively wide range of angles in the forward hemisphere whereas our

data were taken with the detectors subtending a limited angular range near 90°. Hence, angular distribution effects might explain the differences between the two sets of data. However, this does not seem to be a very likely explanation given the generally good agreement observed for previous measurements of the $^{17}O(n,\alpha)^{14}C$ [42,43] and $^{36}Cl(n,p)^{36}S$ [44,45] cross sections, where similar effects were possible, but were not observed to be significant.

For these reasons we believe that the reaction rates calculated from our data are more reliable than those of Ref. [28]. Our results indicate that the total $^{26}Al(n,p)$ reaction rate is at least as large as calculated in Ref. [27]. It is this latter rate which is apparently often used in nucleosynthesis calculations. On the other hand, our results, as well as those of Ref. [25], indicate that the $^{26}Al(n,\alpha)$ given in Ref. [27] is about a factor of 2–3 too small for temperatures below approximately 1 GK.

V. ASTROPHYSICAL IMPLICATIONS

Proposed sites for the origin of significant ^{26}Al include both presupernova and supernova nucleosynthesis in massive stars [8–12], AGB stars [13,5,14,15], W-R stars [16,17], cosmic rays [18,19], and novae [20–23]. The CGRO observations [7] appear to indicate that massive stars are the most likely source of the bulk of the ^{26}Al in our galaxy. Calculations have shown that neutron-induced reactions, most notably $^{26}Al(n,p)$, are the main route for the destruction of ^{26}Al in many scenarios involving massive stars. In addition, these same reactions are calculated to destroy a sizable fraction of the ^{26}Al synthesized in AGB stars.

Most previous nucleosynthesis calculations have used the statistical model rates given in Ref. [27] rather than the rates measured in Refs. [28,25]. The measurements, however, are significantly different from the statistical model calculations. For example, our measurements support a $^{26}Al(n,p)$ rate at least as high as that in Ref. [27] for $T \gtrsim 0.1$ GK. However, at lower temperatures characteristic of the main neutron exposure in low-mass AGB stars ($T \approx 0.07$–0.09 GK), our $^{26}Al(n,p)$ rate is only about 40–50% of the rate in Ref. [27]. Also, our measurements as well as those of Ref. [25] indicate that the rate for the $^{26}Al(n,\alpha)$ reactions is 2–3 times larger than the rate given in Ref. [27] over much of the range of interest to nucleosynthesis calculations.

In these environments, the amount of ^{26}Al produced appears to be roughly inversely proportional to the combined $^{26}Al(n,p)$ plus $^{26}Al(n,\alpha)$ reaction rates. At the temperature characteristic of the major neutron exposure in low-mass AGB stars, the combined rate from Ref. [27] is very close to the experimental rate even though the individual rates are significantly different. This is because the overestimate of the $^{26}Al(n,p)$ rate by the statistical model calculations is nearly compensated by its underestimate of the $^{26}Al(n,\alpha)$ rate. At any rate, nucleosynthesis calculations [15] indicate that the neutron exposure is already much more than is needed to destroy all of the ^{26}Al in this small part of the AGB star, so this component of the destruction appears to be sensitive to only a drastic decrease in the rate compared to Ref. [27]. On the other hand, the measurements indicate that the combined rate at the temperature of the second neutron exposure, due to the (marginal) activation of the $^{22}Ne(\alpha,n)$ neutron source in the convective He shell, is about 30% larger than the theoretical rate of Ref. [27]. This increase in the combined rate should lead to a corresponding decrease in the amount of ^{26}Al produced.

The impact of our measurements on ^{26}Al nucleosynthesis in massive stars is uncertain because there are a variety of zones and processes affecting its destruction by neutrons in these stars and our data do not extend to high enough energies to determine directly the reaction rate at the higher temperatures characteristic of some of these environments. However, our data indicate that the $^{26}Al(n,p)$ rate measured in Ref. [28] is almost a factor of 2 too small. Our measurements together with the shape of the reaction rate measured in Ref. [28] indicate that the theoretical rate of Ref. [27] may be a good approximation of the $^{26}Al(n,p_1)$ rate. When the $^{26}Al(n,p_0)$ data of Ref. [25] and the limits on proton transitions to higher-lying levels in ^{26}Mg are taken into account, the data indicate that the total $^{26}Al(n,p)$ rate is approximately 5–40% larger than that of Ref. [27]. This larger $^{26}Al(n,p)$ rate, combined with fact that the experimentally determined $^{26}Al(n,\alpha_0)$ is factor of 2–3 larger than the rate of Ref. [27], indicates that the ^{26}Al produced by massive stars has probably been overestimated.

VI. CONCLUSIONS

Our measurements of the $^{26}Al(n,\alpha_0)$ and $^{26}Al(n,p_1)$ cross sections as well as previous data [25] indicate that the combined rate for these two reactions has been underestimated in previous nucleosynthesis calculations. Previous calculations indicate that the amount of ^{26}Al produced by massive stars and AGB stars is roughly inversely proportional to this combined rate. As a result, although there are other uncertainties in the models, the amount of ^{26}Al produced has probably been overestimated.

ACKNOWLEDGMENTS

We would like to thank J. C. Gursky for making the ^{6}Li sample used in this experiment, H. A. O'Brien and K. W. Thomas for providing the material for the ^{26}Al sample, and R. M. Mortensen for technical assistance. This work was supported by the U.S. Department of Energy under Contract No. W-7405-end-36 with the University of California (Los Alamos) and Contract No. DE-AC05-96OR22464 with Lockheed Martin Energy Research Corporation (Oak Ridge) and by the National Science Foundation (grant PHY88-17296).

[1] T. Lee, D. A. Papanastassiou, and G. J. Wasserburg, Astrophys. J. **211**, L107 (1977).
[2] E. Anders and E. Zinner, Meteorites **28**, 490 (1993).
[3] U. Ott, Nature (London) **365**, 25 (1993).
[4] D. D. Clayton, Space Sci. Rev. **24**, 147 (1979).
[5] A. G. W. Cameron, Icarus **60**, 416 (1984).
[6] W. A. Mahoney, J. C. Ling, A. S. Jacobson, and R. E. Lingenfelter, Astrophys. J. **262**, 742 (1982).

[7] R. Diehl *et al.*, Astron. Astrophys. **298**, 445 (1995).
[8] J. W. Truran and A. G. W. Cameron, Astrophys. J. **219**, 226 (1978).
[9] W. D. Arnett and J. P. Wefel, Astrophys. J. **224**, L139 (1978).
[10] S. E. Woosley and T. A. Weaver, Astrophys. J. **238**, 1017 (1980).
[11] T. A. Weaver and S. E. Woosley, Phys. Rep. **227**, 65 (1993).
[12] F. X. Timmes, S. E. Woosley, D. H. Hartmann, R. D. Hoffman, T. A. Weaver, and F. Matteucci, Astrophys. J. **449**, 204 (1995).
[13] H. Norgaard, Astrophys. J. **246**, 895 (1980).
[14] M. Forestini, G. Paulus, and M. Arnould, Astron. Astrophys. **252**, 597 (1991).
[15] G. J. Wasserburg, M. Busso, R. Gallino, and C. M. Raiteri, Astrophys. J. **424**, 412 (1994).
[16] M. Signore and C. Dupraz, Astron. Astrophys. **234**, L15 (1990).
[17] M. Signore and C. Dupraz, Astron. Astrophys. Suppl. Ser. **97**, 141 (1993).
[18] D. D. Clayton, Nature (London) **358**, 222 (1994).
[19] D. D. Clayton and L. Jin, Astrophys. J. **451**, L87 (1995).
[20] A. Weiss and J. W. Truran, Astron. Astrophys. **238**, 178 (1990).
[21] I. Nofar, G. Shaviv, and S. Starrfield, Astrophys. J. **369**, 440 (1991).
[22] M. D. Leising, Astron. Astrophys. Suppl. Ser. **97**, 299 (1993).
[23] A. Coc, R. Mochkovitch, Y. Oberto, J. P. Thibaud, and E. Vangioni-Flam, Astron. Astrophys. **299**, 479 (1995).
[24] R. T. Skelton, R. W. Kavanagh, and D. G. Sargood, Astrophys. J. **271**, 404 (1983).
[25] R. T. Skelton, R. W. Kavanagh, and D. G. Sargood, Phys. Rev. C **35**, 45 (1987).
[26] S. E. Woosley, W. A. Fowler, J. A. Holmes, and B. A. Zimmerman, At. Data Nucl. Data Tables **22**, 371 (1978).
[27] G. R. Caughlan and W. A. Fowler, At. Data Nucl. Data Tables **40**, 282 (1988).
[28] H. P. Trautvetter *et al.*, Z. Phys. A **323**, 1 (1986).
[29] K. Brehm, H. W. Becker, C. Rolfs, H. P. Trautvetter, F. Käppeler, and W. Ratynski, Z. Phys. A **330**, 167 (1988).
[30] M. Wiescher, R. Steininger, and F. Käppeler, Astrophys. J. **344**, 464 (1989).
[31] P. E. Koehler and H. A. O'Brien, Phys. Rev. C **39**, 1655 (1989).
[32] J. C. Blackmon, A. E. Champagne, J. K. Dickens, J. A. Harvey, M. A. Hofstee, S. Kopecky, D. C. Larson, D. C. Powell, S. Raman, and M. S. Smith, Phys. Rev. C **54**, 383 (1996).
[33] Y. Nagai, M. Igashira, N. Mukai, T. Ohsaki, F. Uesawa, K. Takeda, T. Ando, H. Kitzaswa, S. Kubono, and T. Fukuda, Astrophys. J. **381**, 444 (1991).
[34] W. L. Imhof, R. G. Johnson, F. J. Vaughn, and M. Walt, Phys. Rev. **114**, 1037 (1959).
[35] P. W. Lisowski, C. D. Bowman, G. J. Russell, and S. A. Wender, Nucl. Sci. Eng. **106**, 208 (1990).
[36] P. E. Koehler, C. D. Bowman, F. J. Steinkruger, D. C. Moody, G. M. Hale, J. W. Starner, S. A. Wender, R. C. Haight, P. W. Lisowski, and W. L. Talbert, Phys. Rev. C **37**, 917 (1988).
[37] R. B. Vogelaar, Ph.D. thesis, Caltech, 1989.
[38] A. D. Carlson, W. P. Poenitz, G. M. Hale, R. W. Peelle, D. C. Dodder, C. Y. Fu, and W. Mannhart, Technical report, National Institute of Standards and Technology Report No. NISTIR-5177 (1993).
[39] P. E. Koehler, Nucl. Instrum. Methods Phys. Res. A **350**, 511 (1994).
[40] P. M. Endt, Nucl. Phys. **A521**, 1 (1990).
[41] N. A. Bahcall and W. A. Fowler, Astrophys. J. **157**, 659 (1969).
[42] P. E. Koehler and S. M. Graff, Phys. Rev. C **44**, 2788 (1991).
[43] H. Schatz, F. Käppeler, P. E. Koehler, M. Wiescher, and H.-P. Trautvetter, Astrophys. J. **413**, 750 (1993).
[44] P. E. Koehler, S. M. Graff, H. A. O'Brien, Y. M. Gledenov, and V. P. Popov, Phys. Rev. C **47**, 2107 (1993).
[45] H. Schatz, S. Jaag, G. Linker, R. Steininger, F. Käppeler, P. E. Koehler, S. M. Graff, and M. Wiescher, Phys. Rev. C **51**, 379 (1995).
[46] P. E. Koehler and H. A. O'Brien, Phys. Rev. C **38**, 2019 (1988).
[47] P. E. Koehler, Phys. Rev. C **44**, 1675 (1991).
[48] R. C. Hanna, Philos. Mag. **46**, 381 (1955).
[49] H. W. Newson, R. M. Williamson, K. W. Jones, J. H. Gibbons, and H. Marshak, Phys. Rev. **108**, 1294 (1957).
[50] R. L. Macklin and J. H. Gibbons, Phys. Rev. **109**, 105 (1958).
[51] J. H. Gibbons and R. L. Macklin, Phys. Rev. **114**, 571 (1959).
[52] H. J. Kim, W. T. Milner, and F. K. McGowan, Nucl. Data, Sect. A **1**, 203 (1966).
[53] Y. M. Gledenov, J. Kvitek, S. Marinova, Y. P. Popov, J. Rigol, and V. I. Salatski, Z. Phys. A **308**, 57 (1982).
[54] M. Sanders, Phys. Rev. **104**, 1434 (1956).
[55] S. Druyts, C. Wagemans, and P. Geltenbort, Nucl. Phys. **A573**, 291 (1994).
[56] R. Bieber, C. Wagemans, J. Heyse, N. Balcaen, R. Barthelemy, and J. V. Gils, in Proceedings of the Conference on Capture Gamma-Ray Spectroscopy and Related Topics (unpublished).